PHYSICAL REVIEW B VOLUME 21, NUMBER 12 15 JUNE 1980

Prediction of Fermi-surface pressure dependence in Rb and Cs

J.-P. Jan and A. H. MacDonald
Division of Physics, National Research Council of Canada, Ottawa, Canada K1A OR6

H. L. Skriver
Risø National Laboratory, DK-4000 Roskilde, Denmark

(Received 20 September 1979)

The linear muffin-tin orbitals method of band-structure calculation, combined with a Gaussian integration technique using special directions in the Brillouin zone, has been used to calculate Fermi radii and extremal cross-sectional areas of the Fermi surface in rubidium and cesium. Band shifts were used to achieve optimum agreement with experimental results. Volume derivatives were then obtained by varying the lattice parameter with the band shifts held constant. The significance of this procedure has been discussed in the light of recent theoretical work. The results obtained for the Fermi-surface pressure dependence agree with the limited experimental data available.

I. INTRODUCTION

The unusual behavior of Cs under compression has attracted theoretical attention to this system.[1-5] Both the first-order isostructural transition at 42.2 kbar[6,7] and the unusual softness of the pressure-volume isotherm[8] at low pressures have been attributed to a shift of the valence electrons from $6s$ orbitals to more localized $5d$ orbitals.[5] [All theoretical treatments have been based on the assumption that the single-particle (band theory) model provides a good description of these metals.] In this article we report a band-theory calculation of the differential changes of the Fermi surface of Cs, and the closely related metal Rb, with small applied pressures. Since the calculations can be performed very accurately and the corresponding experimental quantity should also be susceptible to accurate measurement, the comparison of our results with experiment is a good test of the ability of single-particle theory to account for the pressure dependence of the electronic structure of Cs and Rb in particular, and to a lesser extent of metals in general.

II. COMMENT ON THE BAND-THEORY APPROACH

The Fermi surface of a metal is the locus of points in reciprocal space satisfying $E_{n,\vec{k}}=\mu$ where $E_{n,\vec{k}}$, the quasiparticle energy, is determined by solving the Dyson equation[9]

$$[-\vec{\nabla}^2+v(\vec{r})+v_H(\vec{r})]\psi_{n,\vec{k}}(\vec{r})+\int d\vec{r}\,'M(\vec{r},\vec{r}\,';E_{n,\vec{k}})\psi_{n,\vec{k}}(\vec{r}\,')=E_{n,\vec{k}}\psi_{n,\vec{k}}(\vec{r}) \quad (1)$$

and μ, the chemical potential, satisfies[10]

$$2\sum_{n,\vec{k}}\Theta(\mu-\mathrm{Re}(E_{n,\vec{k}}))=N \ , \quad (2)$$

where Θ is a step function and N the total number of electrons in the system. (We use atomic units with Ry for energy.) In Eq. (1) $M(\vec{r},\vec{r}\,';E)$, the mass operator, is a complicated quantity whose perturbative expansion is given by many-body theory. It is usually approximated by an exchange-correlation potential as follows:

$$\int d\vec{r}\,'M(\vec{r},\vec{r}\,';E)\psi_{n,\vec{k}}(\vec{r}\,')\simeq v_{\mathrm{xc}}(\vec{r})\psi_{n,\vec{k}}(\vec{r}) \ , \quad (3)$$

with a number of different but similar approximations for v_{xc} in common use.[11-14] Equation (3) is the essential approximation of the band theory for electronic structure.

In this work we have adopted the muffin-tin approximation and, for the most part, used the Mattheiss[15] prescription for generating the crystal potential. The resulting single-particle equations were solved using the accurate, but approximate, linear muffin-tin orbitals (LMTO) method due to Andersen.[16] With these approximations, the zero pressure Fermi surface of Cs was determined for the two extreme v_{xc}, $X\alpha$ potentials with $\alpha=1$ and $\frac{2}{3}$. Comparison of these Fermi surfaces with the accurately known experimental Fermi surfaces determined by

Gaertner and Templeton[17] showed that neither choice of α could yield accurate theoretical Fermi surfaces. Since the Fermi surface will be a smooth function of α it was clear that none of the commonly used approximations for v_{xc} would yield accurate Fermi surfaces. Moreover, as will be discussed later, self-consistency worsened the agreement between theory and experiment and non-muffin-tin corrections have no significant effect on the Fermi surface of Rb,[18] or presumably Cs. It is clear that Eq. (3) is responsible for the discrepancy. Therefore, the zero pressure crystal potential was modified by a small phenomenological nonlocal correction $\Delta U(\vec{r},\vec{r}')$, the form of which is discussed in the next section. Essentially, we have adjusted the crystal potential so that it produces phase shifts which yield agreement with the experimental Fermi surface. Similar approaches have been taken previously by others[19–21] but the validity of phase-shift Fermi-surface fits has recently been questioned by Wang and Rasolt.[22] We therefore attempt to clarify the significance of our approach to this calculation in the following paragraph.

It is usually claimed that phase-shift adjustments account for the nonlocality of $M(\vec{r},\vec{r}';\mu)$. However, it can be shown that only nonlocal forms which satisfy the requirement that $M(\vec{r},\vec{r}';\mu)=0$ for $\vec{r}$ and $\vec{r}'$ in *different* atomic spheres can be incorporated exactly into the LMTO method by a simple modification of the phase shifts. A similar comment applies to phase-shift adjustments within (augmented plane wave) (APW), Korringa-Kohn-Rostoker (KKR), and other similar methods. Wang and Rasolt[22] have pointed out that, at least for simple metals, no form satisfying this restriction can adequately approximate $M(\vec{r},\vec{r}';\mu)$. Nevertheless our success in fitting the observed Fermi surfaces, and previous experience,[19–21] demonstrates that we can find forms such that

$$\int d\vec{r}'\,\Delta U(\vec{r},\vec{r}')\psi_{n,\vec{k}}(\vec{r}') \simeq \int d\vec{r}'\,[M(\vec{r},\vec{r}';\mu)-\delta(\vec{r}-\vec{r}')v_{xc}(\vec{r})]\psi_{n,\vec{k}}(\vec{r}') \tag{4}$$

for electrons on the Fermi surface. This is all that is required for a Fermi-surface calculation but it should be remembered that the phenomenologically determined $\Delta U(\vec{r},\vec{r}')$ gives no information about the nonlocality of $M(\vec{r},\vec{r}';\mu)$.

To calculate the pressure dependence of the Fermi surfaces we have selected from reasonable choices for $v_{xc}(\vec{r})$, that which requires the smallest $\Delta U(\vec{r},\vec{r}')$ in order to bring the zero pressure Fermi surface into agreement with experiment. The pressure dependence of $\Delta U(\vec{r},\vec{r}')$ is then assumed to be negligible compared to that of $U(\vec{r},\vec{r}')$ as a whole and the kinetic energy of the metal in calculating the changes of the Fermi surfaces with lattice constant. We believe that the procedure described above is a reasonable one for approximating the pressure dependence of the Fermi surfaces of metals by band theory. Since there is no practical alternative to band theory for predicting the pressure dependence of the Fermi surfaces of metals, we believe that the comparison of these calculations with appropriate experiment provides an accurate measure of the ability of present theory to explain this aspect of the electronic structure of metals.

III. METHOD OF CALCULATION

As mentioned in the previous section the single-particle equations in this work were solved by the LMTO method. In this method, the logarithmic derivatives $D_l(E)$, of the radial wave functions at the atomic sphere radius S are parametrized by the following equation:

$$[D_l(E)-D_l]^{-1} = -[m_l S^2(E-E_l)]^{-1} + a_l + b_l S^2(E-E_l) \ , \tag{5}$$

where E_l is a reference energy for the truncated Laurent expansion and $D_l = D_l(E_l)$, m_l, a_l, and b_l are the four potential parameters for each partial wave. The calculated $D_l(E)$ included the relativistic mass-velocity and Darwin corrections since they were obtained by solving the radial Dirac equation and following the prescription suggested by Andersen[16] rather than by solving the Schrödinger equation. Furthermore, the calculation goes beyond the atomic sphere approximation in that the combined correction terms are employed.[16] The phenomenological potential correction is chosen to take the form

$$\Delta U(\vec{r},\vec{r}') = \sum_l \Delta E_l \Theta(S-r)\hat{p}_l \ , \tag{6}$$

where $\hat{P}_l$ is the partial-wave projection operator inside an atomic sphere containing $\vec{r}$ and $\vec{r}'$ and r is the distance from the center of that muffin-tin sphere. The parameters of $\Delta U(\vec{r},\vec{r}')$, the l-dependent energy shifts ΔE_l, are very convenient to use in conjunction with the LMTO method since they merely result in the replacement of the reference energy E_l which appears in Eq. (6) by $E_l' = E_l + \Delta E_l$. Since the theoretical Fermi surface was found to depend smoothly on the shift parameters $\{\Delta E_l\}$ calculations for several trial cases made it possible to choose shift values which yielded close fits to the experimental Fermi surface.

We now discuss the method used to determine the Fermi surface. For the case of the simply connected Fermi surfaces Eq. (2) can be written in the simplified form

$$\int \frac{d\hat{\Omega}}{4\pi}\left[\frac{k_F(\hat{\Omega})}{k_F^0}\right]^3 \equiv N(\mu)=1 \ , \tag{7}$$

where k_F^0 is the Fermi wave vector for the free-electron system with the same valence electron density, and $k_F(\hat{\Omega})$ is the Fermi wave vector in direction $\hat{\Omega}$. The integral over solid angle in Eq. (7) was evaluated using the powerful Gaussian direction integration formulas derived by Fehlner *et al.*[23] and by Fehlner and Vosko[24]; their 21-direction formula was used in this work. Thus given a guess for μ, $N(\mu)$ was evaluated from Eq. (7) and then μ was varied until $|N(\mu)-1|<10^{-5}$. With μ fixed $k_F(\hat{\Omega})$ was given by

$$k_F^2(\hat{\Omega})=(k_F^0)^2\sum_{L,d}\gamma_{L,d}K_{L,d}(\hat{\Omega}) \ , \tag{8}$$

where $K_{L,d}(\hat{\Omega})$ are the Kubic harmonics in the notation of Fehlner and Vosko[24] and the expansion coefficients, $\{\gamma_{L,d}\}$ were determined from the Gaussian direction integration formulas as follows[23]:

$$\gamma_{L,d}=\sum_i W_i K_{L,d}(\hat{\Omega}_i)[k_F(\hat{\Omega}_i)/k_F^0]^2 \ . \tag{9}$$

In Eq. (9) $\{\hat{\Omega}_i\}$ are the Gaussian directions and $\{W_i\}$ are the corresponding weights. Furthermore, the extremal cross-sectional area of the Fermi surface in planes perpendicular to $\hat{\Omega}$, $A(\hat{\Omega})$, the quantity most directly measured in a de Haas-van Alphen experiment, is also given in terms of $\gamma_{L,d}$ by[25]

$$A(\hat{\Omega})=A^0\sum_{L,d}P_L(0)\gamma_{L,d}K_{L,d}(\hat{\Omega}) \ , \tag{10}$$

where $A^0=\pi(k_F^0)^2$ is the cross-sectional area of the free-electron Fermi sphere. For Rb we retained all Kubic harmonics with $L\lesssim 14$ while for Cs those with $L\lesssim 16$ were retained. The error in determining $A(\hat{\Omega})$ and $k_F(\hat{\Omega})$ in a given direction from the eigenvalues along the Gaussian directions was estimated to be several parts in 10^4. On the other hand the Fermi-surface distortions from sphericity obtained when the free-electron test was applied to the LMTO method were as much as one part in 10^3. Thus the accuracy of the eigenvalue determination, although partially corrected for by the adjustment of the zero pressure potential, was the limiting factor in the accuracy of this calculation.

IV. RESULTS AND DISCUSSION

A. Zero pressure results

The Fermi radius and extremal area distortions for high-symmetry directions as calculated from several potentials are compared with experiment in Table I. For the $\alpha=\frac{2}{3}$ and 1 calculations the potentials were

TABLE I. Comparison of starting potentials.

		Local dens. self-cons.	$\alpha=1$	$\alpha=\frac{2}{3}$	$\alpha=\frac{2}{3}$ shifted	Experiment[a]
Rubidium						
	⟨100⟩	· · ·	· · ·	45	48	42
$(10^4)\Delta A/A_0$	⟨110⟩	· · ·	· · ·	−25	−26	−27
	⟨111⟩	· · ·	· · ·	47	51	59
	⟨100⟩	· · ·	· · ·	−14	−14	−12
$(10^4)\Delta k/k_0$	⟨110⟩	· · ·	· · ·	96	103	99
	⟨111⟩	· · ·	· · ·	−47	−51	−56
Cesium						
	⟨100⟩	313	254	250	147	131
$(10^4)\Delta A/A_0$	⟨110⟩	−152	−142	−136	−94	−90
	⟨111⟩	613	518	426	242	253
	⟨100⟩	−261	−235	−168	−101	−89
$(10^4)\Delta k/k_0$	⟨110⟩	1033	861	730	413	418
	⟨111⟩	−349	−302	−284	−183	−184

[a]Reference 17.

TABLE II. Crystal potential data for Rb and Cs (Bohr radius = 0.52917706 Å).

	Rb	Cs
"dHvA" lattice parameter (Å) (Ref. 17)	5.588	6.041
Muffin-tin zero E_{MTZ} (Ry)	−0.384	−0.369
Muffin-tin radius S_{MT} (a.u.)	4.4817	4.7115
Potential discontinuity at S_{MT}, Δ_{MT} (Ry)	0.025	0.030
Free-electron area A_0 (a.u.)	0.42803	0.36624
Free-electron Fermi radius k_0 (a.u.)	0.36912	0.34144
Fraction of volume occupied by muffin-tin spheres	64.0%	58.9%

generated by the Mattheiss[15] prescription with the neutral-atom charge densities calculated by the Dirac-Slater method using the same value of α. As is clear from Table I the higher α value gives a more distorted Fermi surface; this is expected since a higher α value will lower the more localized d orbitals relative to the s-p orbitals. Also shown in Table I is the Fermi surface implied by a self-consistent calculation on Cs using the Hedin-Lundqvist[13] exchange-correlation potential. At the valence electron density of Cs this potential corresponds roughly to $\alpha(r_s) \sim 0.9$ and, as is clear from the table, the usual increase of the effective value of α with self-consistency is evidenced. For Cs, the $\alpha = \frac{2}{3}$ Fermi surface was best but still more than twice as distorted as the experimental Fermi surface while for Rb the $\alpha = \frac{2}{3}$ potential gave excellent results so that no other potentials were tried. The energy shifts $\{\Delta E_l\}$ were determined by varying them systematically until we minimized the sum of the squares of the differences between the calculated and observed values of the following six quantities: $\Delta A/A_0$ and $\Delta k/k_0$ in the three principal crystallographic directions, $\langle 100\rangle$, $\langle 110\rangle$, and $\langle 111\rangle$. ($\Delta A \equiv A - A^0$ and $\Delta k \equiv k - k_F^0$.) Results for this shifted potential also appear in Table I. Note that the absolute discrepancies between our best fit and experiment are comparable in Rb and Cs, but the relative discrepancies are much larger in Rb because its Fermi surface is considerably less distorted than that of Cs. A comparison between best fit and experiment for the {100} and {110} planes is shown in Figs. 5–8.

It should be noted that in Ref. 17, hereafter referred to as GT, A^0 and k_F^0 are based on Barrett's values of the lattice spacing at 5 K[26]; they are used as convenient reference values but do not rigorously correspond to a one-electron sphere. We have preferred to use the slightly different de Haas-van Alphen parameters given by GT (their Table VI) which are based on their calculation of the Fermi-surface volume. In Table I the values of ΔA and Δk listed by GT have been modified for the resulting change of A^0 and k_F^0.

In the LMTO method the crystal potential is conveniently summarized by the potential parameters defined by Eq. (5); these parameters are listed in Table III for Rb and Cs. (Table II lists some data related to the construction of the crystal potential.) In each

TABLE III. Central potential parameters for rubidium and cesium at normal pressure ($\alpha = \frac{2}{3}$).

	Rubidium			Cesium		
Atomic sphere radius S (a.u.)		5.1994			5.6208	
	5s	5p	4d	6s	6p	5d
C_l (Ry above E_{MTZ} unshifted)	0.1055	0.4258	0.4584	0.1070	0.4047	0.3597
Shift ΔC_l (Ry)	0.0	−0.0007	−0.0025	0.0	0.0062	0.0239
$\mu_l \equiv 2m_l(C_l)$	0.811	0.853	2.267	0.772	0.802	2.378
a_l	0.1571	0.1307	0.1805	0.1503	0.1241	0.1751
$100b_l$	0.263	0.175	0.481	0.235	0.156	0.423
ξ_l (mRy)		8.7	0.9		19.8	2.3
$\omega_l(D^l)$ (Ry)		−1.613	−0.431		−1.737	−0.419
$S^2(C_l - C_s)$ unshifted		8.66	9.54		9.41	3.38
$S^2(C_l - C_s)$ free el.		7.4	17.7		7.4	17.7

TABLE IV. Miscellaneous band and density-of-states data.

	Rb	Cs
Fermi level E_F above E_{MTZ} (Ry)	0.1554	0.1544
Gap at $N.E(N_1)-E(N_1')$ (Ry)	−0.0436	−0.0642
Density of states $N(E_F)$ (electron cell^{-1} Ry^{-1})	11.62	15.05
Electronic specific-heat coefficient γ (mJ mol^{-1} K^{-2})	2.012	2.608
Free electron $\gamma=\gamma_0$	1.907	2.229
Band thermal mass γ/γ_0	1.06	1.17
Experimental thermal mass (Ref. 27)	1.37±0.01	1.80±0.04
Experimental cyclotron mass	1.260±0.001[a]	1.4−1.5[b]

[a]Reference 29. [b]Reference 17.

case we have chosen the reference energy for each partial wave to be the center of the corresponding band C_l, defined by $D_l(C_l)=-l-1$. The band shifts are also shown in this table. In practice we have not shifted the s band since a uniform shift of all three bands merely redefines the zero of energy. The major band shift is a raising of the d band in Cs by about 24 mRy. This reduces the excessive Fermi-surface distortion occurring with the unshifted bands. In Rb the shifts are almost negligible. Table III also lists the two parameters ξ_l and ω_l which describe respectively the spin-orbit splitting at the center of the band and its energy dependence (see Andersen).[16] Spin-orbit corrections were included in Cs but were found to have a negligible effect on the Fermi surface; the smaller spin-orbit effects in Rb were dropped.

Miscellaneous band data for thee zero pressure potentials are listed in Table IV. A quantity of interest in pseudopotential calculations is the s-p gap between states N_1 and N_1' and this is larger in Cs as expected. Also interesting is the Fermi-level density of states. As was pointed out by GT there exists a discrepancy between the quasiparticle effective masses in Rb and Cs inferred from de Haas-van Alphen and specific-heat[27] experiments. Our Fermi-level density of states mass, when multiplied by a reasonable estimate of the electron-phonon mass enhancement of ~1.15 ±.05 (Ref. 28) appears to favor the de Haas van Alphen values.[29]

The actual bands for Rb and Cs are shown in Figs. 1 and 2 and the densities of states, including the partial s, p, and d contributions are presented in Figs. 3 and 4. Spin-orbit splitting has not been included in the calculations for these four figures.

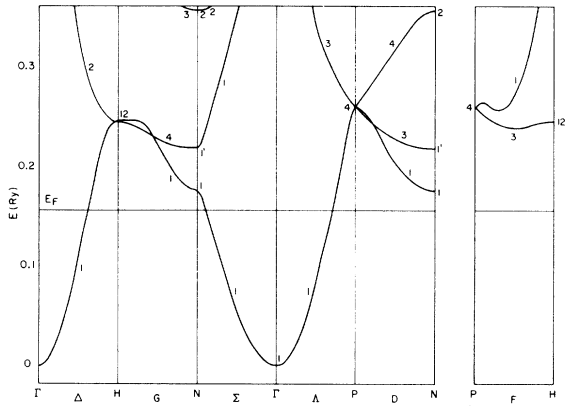

FIG. 1. LMTO bands for rubidium (without spin-orbit splitting).

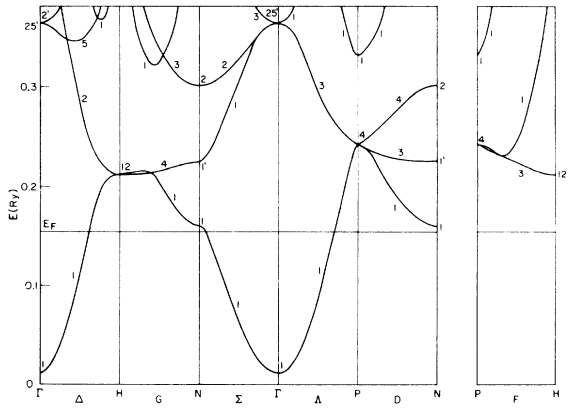

FIG. 2. LMTO bands for cesium (without spin-orbit splitting).

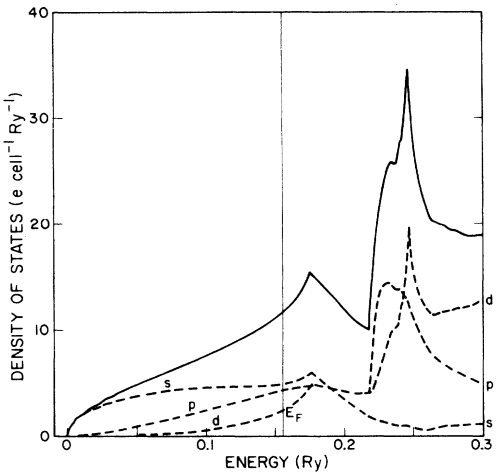

FIG. 3. Total (solid line) and decomposed (dashed lines) densities of states for rubidium. This calculation corresponds to the bands of Fig. 1.

B. Pressure dependent results

The direct results of experiments are the pressure derivatives $d\ln A/dp$ and perhaps $d\ln k/dp$ if a suitable inversion scheme can be used to get Fermi radii. We have calculated $d\ln(A/A_0)/d\ln a$ and $d\ln(k/k_0)/d\ln a$ using variations of $\pm 1\%$ in the lattice parameter a. These two quantities represent the changes in Fermi-surface distortions only, and do not reflect the trivial scaling of reciprocal space with lattice constant. These quantities are related to the pressure derivatives by the equations

$$d\ln(A/A_0)/d\ln a = -(3/K)d\ln A/dp + 2 \quad , \quad (11)$$

$$d\ln(k/k_0)/d\ln a = -(3/K)d\ln k/dp + 1 \quad , \quad (12)$$

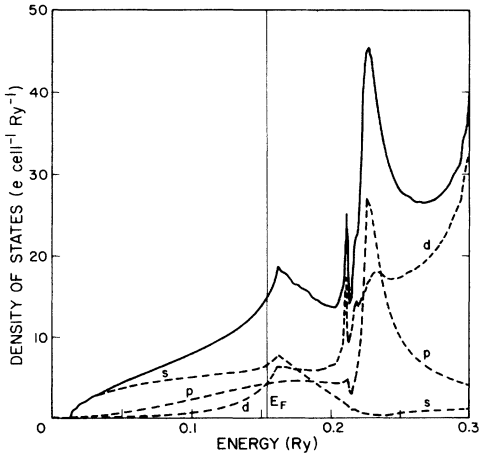

FIG. 4. Total (solid line) and decomposed (dashed lines) densities of states for cesium. This calculation corresponds to the bands of Fig. 2.

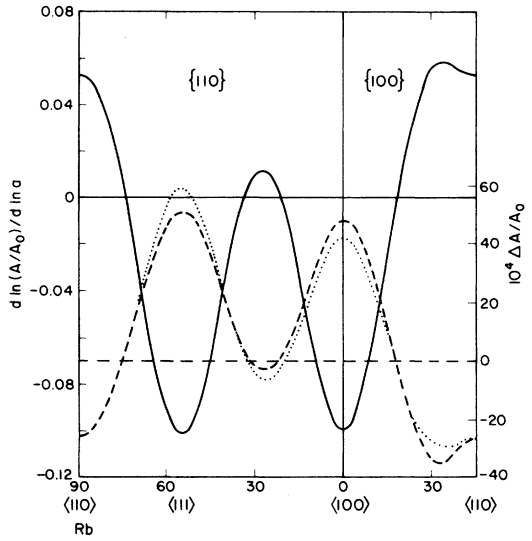

FIG. 5. Area derivatives for rubidium (solid line), and area distortion at normal pressure: 10 Kubic harmonic calculation (dashed line), experimental results from Ref. 17 (dotted line).

where K is the compressibility.

The calculated change in distortion is somewhat larger for the 1% contraction than for the 1% expansion; the finite difference chosen already take us outside the linear range. For instance, for Rb in the ⟨110⟩ direction, $d\ln(A/A_0)/d\ln a$ is 0.056 from the -1% change in a and 0.048 from the $+1\%$ change in a. In Figs. 5–8 we have plotted the average between the two results, together with the calculated and ob-

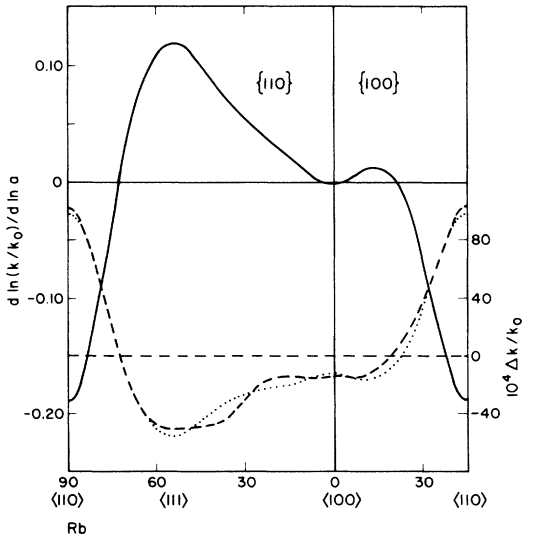

FIG. 6. Fermi-radius derivatives for rubidium (solid line) and Fermi-radius distortion at normal pressure: 10 Kubic harmonic calculation (dashed line), experimental results from Ref. 17 (dotted line).

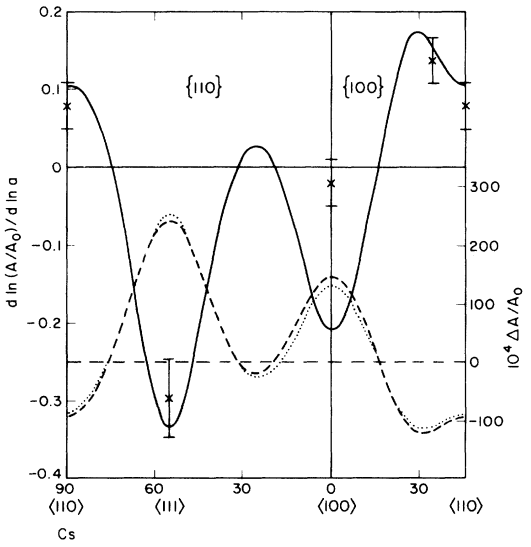

FIG. 7. Area derivatives for cesium (solid line) with experimental results of Ref. 27 (X); area distortion at normal pressure: 8 Kubic harmonic calculation (dashed line), experimental results from Ref. 17 (dotted line).

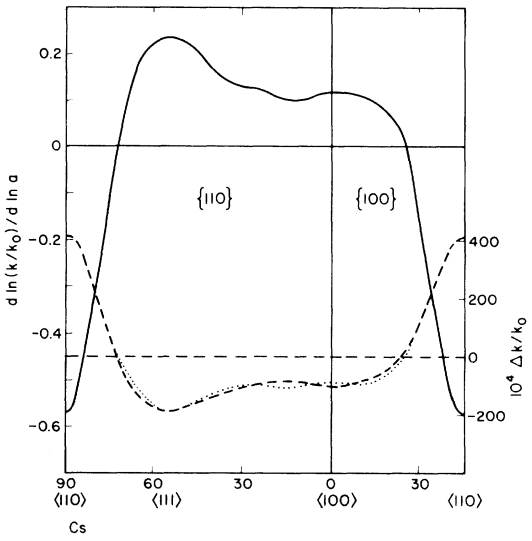

FIG. 8. Fermi-radius derivatives for cesium (solid line) and Fermi-radius distortion at normal pressure: 8 Kubic harmonic calculation (dashed line), experimental results from Ref. 17 (dotted line).

served GT area and radius distortions at zero pressure, for the {100} and {110} planes. An inspection of the angular dependence shows that the size of the Fermi-surface distortion is predicted to increase when the lattice parameter is decreased, while the shape of the distortion is not greatly altered (i.e., $d\ln(A/A_0)/d\ln a \propto \Delta A/A_0$). Both these results are expected since the physical mechanism which produces the distortions at zero pressure (i.e., the proximity of a relatively localized d band) is exactly what is increased in importance by applied pressure (see below).

These results can be interpreted in terms of the behavior of the parameters B_l, C_l, and A_l with applied pressure. Defined by $D_l(B_l)=0$, $D_l(C_l)=-l-1$, and $D_l(A_l)=-\infty$ these parameters represent, respectively, the bottom, middle, and top of the bands corresponding to the lth partial wave. As indicated in Table V, at zero pressure the middle of the s band lies slightly below the Fermi level while the bottom of the p and d bands are still above the Fermi level. The partial densities of states shown in Figs. 3 and 4 are qualitatively in accord with this observation. The closer proximity of the d band in Cs is responsible for the larger Fermi-surface distortion in that case. As pressure is applied the free-electron-like s and p bands broaden much more rapidly than the more localized d band (see Table V). As a result the bottom of the d band moves closer to the Fermi level. This is the cause of the increase in distortion with applied pressure in both Rb and Cs.

The only existing experimental results we are

TABLE V. Position of shifted unhybridized bands relative to the Fermi level and their derivatives (in Ry).

	Rb s	Rb p	Rb d	Cs s	Cs p	Cs d
Bottom B_l	−0.1572	0.0408	0.1122	−0.1431	0.0513	0.0773
Center C_l	−0.0499	0.2697	0.3006	−0.0474	0.2565	0.2292
Top A_l	0.3962	0.7905	0.4591	0.3706	0.7524	0.3645
$dB_l/d\ln a$	0.33	−0.16	0.14	0.26	−0.25	0.18
$dC_l/d\ln a$	0.03	−0.70	−0.25	−0.02	−0.75	−0.22
$dA_l/d\ln a$	−1.50	−2.24	−0.65	−1.52	−2.27	−0.64

TABLE VI. Comparison of calculated and observed pressure derivatives in cesium.

Direction	$d\ln A/dp$[a] (% kbar^{-1})	$d\ln(A/A_0)/d\ln a$ observed[b]	calculated
⟨100⟩	2.90±0.05	−0.02±0.03	−0.21
⟨110⟩	2.75±0.05	0.08±0.03	0.10
⟨111⟩	3.30±0.07	−0.30±0.05	−0.34
11° from ⟨110⟩ in {100}	2.67±0.05	0.14±0.03	0.16

[a]Observed by Beardsley and Schirber (Ref. 30). [b]From Eq. (18) using $K=0.043$ kbar^{-1}.

aware of which allow a direct comparison with our calculation are those of Beardsley and Schirber[30] on Cs. These results are shown in Table VI. The compressibility we used to calculate $d\ln(A/A_0)/d\ln a$ from Eq. (11), $K=0.043$ kbar^{-1}, will be discussed later. The uncertainties quoted on the observed area derivatives do not include any uncertainty on K. [Use of a different K in Eq. (11) would shift the four observed values uniformly up or down.] The agreement is excellent at ⟨110⟩, 11° from ⟨110⟩ and at ⟨111⟩ but very poor at ⟨100⟩ where the observations give no change in distortion within experimental error. We note that this observation is also at odds with the expected proportionality of $d\ln(A/A_0)/d\ln a$ and $\Delta A/A_0$. While further experiments are necessary to provide a more definitive test of our calculations, the agreement between theory and experiment at the other three orientations would tend to indicate that the observation at this orientation is in error.

We have estimated how much compression is required for the Cs Fermi surface to contact the zone boundary at N. A band calculation was done at a lattice spacing decreased by 4%. The four results, at lattice changes of +1%, 0%, −1%, and −4% were extrapolated with a cubic, predicting contact at −6.7% lattice change. We did not calculate bands for this sort of distortion, because below −4.8% our muffin-tin spheres, which have a constant radius, would overlap. Contact would then occur at a lattice spacing of 5.636 Å. If we accept a room-temperature lattice spacing of 6.175 Å (quoted by Ham[2]), a volume reduction $V/V_0=0.76$ is required at that temperature to give contact. Bridgman[31] found a minimum in the electrical resistivity of cesium at $V/V_0\simeq 0.83$. This minimum has been associated with contact or approach to contact, and this makes our result look quite reasonable.

C. Compressibility measurements from de Haas-van Alphen data

Some years ago, Glinski and Templeton[32] determined the change in de Haas-van Alphen area in samples of K, Rb, and Cs under hydrostatic pressure. They calculated an "area compressibility" K_A from the formula

$$K_A=\tfrac{3}{2}d\ln A/dp \quad . \tag{13}$$

Since the true compressibility K is given by

$$K=\tfrac{3}{2}d\ln A_0/dp \quad , \tag{14}$$

the two quantities K and K_A are related by the formula

$$K=K_A/[1-\tfrac{1}{2}d\ln(A/A_0)/d\ln a] \quad . \tag{15}$$

Glinski and Templeton assumed that they could neglect the change in Fermi-surface distortion with pressure; this assumption leads to $K=K_A$, which they found to yield systematically lower values than were obtained by other methods (pVT, ultrasonic). Beardsley and Schirber[30] pointed out that the pressure distortion could not be neglected, and supported this statement by measurements on four oriented single crystals of cesium. They used an averaging formula to obtain a compressibility of 0.044 ±0.002 kbar^{-1}.

If we accept our theoretical prediction for $d\ln(A/A_0)/d\ln a$, we can reinterpret the data of Beardsley and Schirber as follows. Equation (15) can be used to calculate K from the observed K_A, and the resulting K should be independent of orientation. The results are shown in Table VII. Three values of

TABLE VII. Compressibility of cesium (in % kbar^{-1}) obtained by interpreting the results of Ref. 30 in the light of the present calculation.

Direction	K_A Ref. 30	K Eq. (22)
⟨100⟩	4.35	3.93
⟨110⟩	4.13	4.34
⟨111⟩	4.95	4.24
11° from ⟨110⟩ in {100}	4.01	4.35

TABLE VIII. Interpretation of the results of Ref. 32 on the compressibility of Rb and Cs (in % kbar^{-1}).

Sample	K_A	K from Eq. (22)
Rb-$P2$	3.165	3.21 ± 0.02
Cs-$P1$	4.037	4.16 ± 0.04
Cs-$P2$	4.002	4.18 ± 0.04

K are quite compatible, but the value at ⟨100⟩ is outside the error margin (uncertainties on the pressure derivatives are about 2%). If we reject this point, we find an average of 0.043 ± 0.001 kbar^{-1}, which was used in the preceding section. We have, in a sense, treated the compressibility as an adjustable parameter, and the value chosen is the one that fits our theoretical predictions best.

We shall now try to reinterpret the results of Glinski and Templeton. Unfortunately, the crystallographic orientation of their samples is no longer available. Their paper, however, lists the values of $\Delta A/A_0$ for each sample. This leads us to examine the previously mentioned correlation between $d \ln(A/A_0)/d \ln a$ and $\Delta A/A_0$ more closely. If we plot the former quantity as a function of the latter for the {100} and {110} planes, all points fall roughly on a straight line of negative slope going through the origin. Assuming that this correlation holds for any orientation, we can obtain $d \ln(A/A_0)/d \ln a$ from $\Delta A/A_0$ and then K from Eq. (15). The results of this analysis are listed in Table VIII. The two values of K for Cs are quite compatible. The error margin takes into account uncertainties on the correlation discussed above.

Finally, in Table IX, we summarize the available data on the compressibilities. This shows that the pVT results tend to be systematically high but all other results are quite compatible.

D. Phase shifts

Starting from the potential parameters, it is possible to calculate the phase shifts for the three partial waves at the Fermi level. The results are in excellent agreement with the phase shifts calculated by Coleridge[33] using the recent data of Ref. 17. This is expected since, as mentioned previously, our approach at zero pressure is equivalent to a phase-shift fit.

TABLE IX. Summary of compressibilities for Rb and Cs (in % kbar^{-1}).

	Rb	Cs
pVT quoted by Ref. 32[a]	3.45	4.65 ± 0.22
Ultrasonic quoted by Ref. 32[a]	3.27	4.33 ± 0.33
dHvA Ref. 32[b]	3.21 ± 0.02	4.17 ± 0.04
dHvA Ref. 30		4.4 ± 0.2
dHvA Ref. 30 present interpretation		4.3 ± 0.1

[a]Uncertainties for Cs estimated in Ref. 30.
[b]Corrected for orientation (see text).

V. CONCLUSIONS

We have shown that the LMTO method of band-structure calculation can accurately describe the observed Fermi surfaces of rubidium and cesium. The nonlocality of the potential was simulated by a suitable shift of the p and d bands; an attempt was made to clarify the significance of this procedure. We have made detailed predictions concerning the volume derivatives of the extremal Fermi-surface areas and of the Fermi radii. They are compatible with the limited data available indicating that present theory can accurately account for the pressure dependence of the electronic structure of these metals. We hope that this calculation will stimulate detailed measurements of the pressure derivatives as a function of orientation, which are technically feasible with sufficient accuracy at the present time.

ACKNOWLEDGMENTS

The authors are grateful to the following people for advice and discussions: Dr. P. T. Coleridge, Dr. A. A. Gaertner, and Dr. I. M. Templeton. Dr. Gaertner and Dr. Templeton also kindly supplied computer printouts of detailed results of Ref. 17.

[1]F. S. Ham, Phys. Rev. 128, 82 (1962).
[2]F. S. Ham, Phys. Rev. 128, 2524 (1962).
[3]J. Yamashita and S. Asano, J. Phys. Soc. Jpn. 29, 264 (1970).
[4]S. J. Louie and M. L. Cohen, Phys. Rev. B 10, 3237 (1974).
[5]A. K. McMahan, Phys. Rev. B 17, 1521 (1978).
[6]H. T. Hall, L. Merrill, and J. D. Barnett, Science 146, 1297 (1964).
[7]D. B. McWhan, G. Parisot, and D. Bloch, J. Phys. F 4, L69 (1974).
[8]M. S. Anderson, E. J. Gutman, J. R. Packard, and C. A. Swenson, J. Phys. Chem. Solids 30, 1587 (1969).
[9]A. H. MacDonald, J. Phys. F 9, L99 (1979).
[10]J. M. Luttinger, Phys. Rev. 119, 1153 (1960).
[11]W. Kohn and L. J. Sham, Phys. Rev. 140, A1133 (1965).
[12]L. J. Sham and W. Kohn, Phys. Rev. 145, 561 (1966).
[13]L. Hedin and B. I. Lundqvist, J. Phys. C 4, 2064 (1971).
[14]A. H. MacDonald, M. W. C. Dharma-wardana, and D. J. W. Geldart, J. Phys. F (to be published). This paper contains convenient parametrizations of $\alpha(r_s)$ corresponding to several different approximations for the electron-gas chemical potential.
[15]L. F. Mattheiss, Phys. Rev. 133, A1399 (1964).
[16]O. K. Andersen, Phys. Rev. B 12, 3060 (1975).
[17]A. A. Gaertner and I. M. Templeton, J. Low Temp. Phys. 29, 205 (1977).
[18]G. S. Painter, J. S. Faulkner, and G. M. Stocks, Phys. Rev. B 9, 2448 (1974).
[19]B. Segall and F. S. Ham, in *Methods in Computational Physics. Energy Bands in Solids*, edited by B. Alder, S. Fernbach, and M. Rosenberg (Academic, New York, 1968), Vol. 8, Chap. 7.
[20]M. J. G. Lee, Phys. Rev. 178, 953 (1969).
[21]A. B. Chen and B. Segall, Phys. Rev. B 12, 600 (1975).
[22]J. S. Wang and M. Rasolt, Phys. Status. Solidi. B 86, 37 (1978).
[23]W. R. Fehlner, S. B. Nickerson, and S. H. Vosko, Solid State Commun. 19, 83 (1976).
[24]W. R. Fehlner and S. H. Vosko, Can. J. Phys. 54, 2159 (1976).
[25]F. M. Mueller, Phys. Rev. 148, 636 (1966).
[26]C. S. Barrett, Acta Crystallogr. 9, 671 (1956).
[27]D. L. Martin, Can. J. Phys. 48, 1327 (1970).
[28]G. Grimvall, Phys. Scr. 14, 63 (1976).
[29]D. McK. Paul and M. Springford, J. Phys. F 8, 1713 (1978).
[30]G. M. Beardsley and J. E. Schirber, J. Low Temp. Phys. 8, 421 (1972).
[31]P. W. Bridgman, Proc. Am. Acad. Arts Sci. 60, 385 (1925). See also, J. S. Dugdale and D. Phillips, Proc. R. Soc. London Ser. A 287, 381 (1965).
[32]R. Glinski and I. M. Templeton, J. Low Temp. Phys. 1, 223 (1969).
[33]P. T. Coleridge (private communication).